RSC Advances

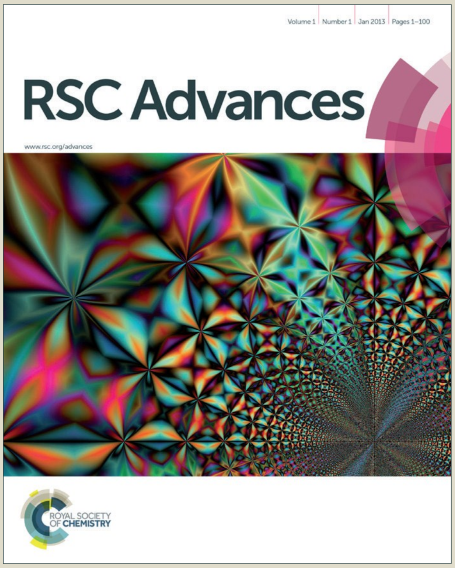

ROYAL SOCIETY OF CHEMISTRY

www.rsc.org/advances

Highly selective and sensitive fluorescence optode membrane for uranyl ion based on 5-(9-anthracenylmethyl)-5-aza-2,8-dithia[9],(2,9)-1,10-phenanthrolinophane

Mojtaba Shamsipur, Moslem Mohammadi, Avat (Arman) Taherpour, Alessandra Garau and Vito Lippolis

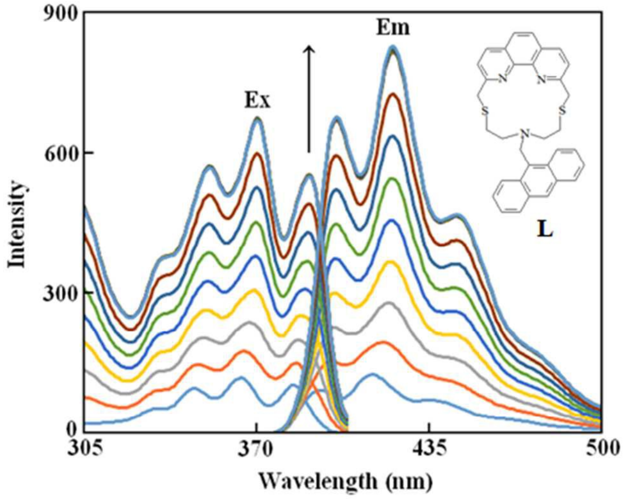

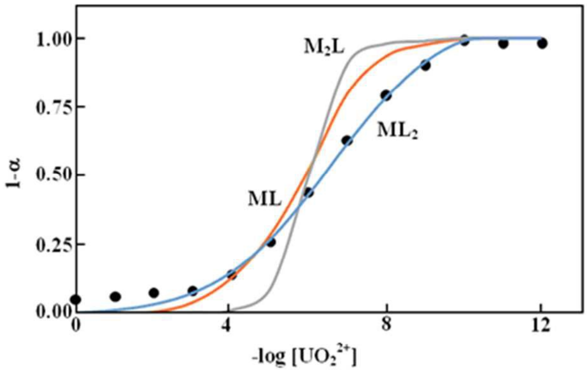

A highly sensitive and selective fluorimetric optode membrane based on the enhancement in fluorescence emission of 5-(9-anthracenylmethyl)-5-aza-2,8-dithia[9],(2,9)-1,10-phenanthrolinophane (**L**) at 425 nm (λ_{ex} = 366 nm) for subnanomolar detection of uranyl ion is described is presented.

Highly selective and sensitive fluorescence optode membrane for uranyl ion based on 5-(9-anthracenylmethyl)-5-aza-2,8-dithia[9],(2,9)-1,10-phenanthrolinophane

Mojtaba Shamsipur,*[a] Moslem Mohammadi,[a] Avat (Arman) Taherpour,[a] Alessandra Garau[b] and Vito Lippolis[b]

A highly selective and sensitive fluorescent sensor for the determination of uranyl ion is developed. The sensing membrane was prepared by incorporating 5-(9-anthracenylmethyl)-5-aza-2,8-dithia[9],(2,9)-1,10-phenanthrolinophane as fluoroionophore in the plasticized poly(vinyl chloride) membrane containing 2-nitrophenyloctylether as plasticizer. The proposed sensor displays a wide linear response range of 1.0×10^{-10}–1.0×10^{-3} M with a low limit of detection of 2.7×10^{-11} M in solution at pH 4.0. This sensor has a relatively fast response time of less than three min. In addition to high stability and reproducibility, it shows a unique selectivity towards uranyl ion with respect to common coexisting cations. The sensor can be regenerated by exposure to a solution of ethylene diamine tetraacetic acid. The proposed sensor was then applied to the determination of uranyl in water samples with satisfactory results.

Keywords: Optical sensor; Uranyl; PVC membrane; Fluorescence spectroscopy.

---

[a] *Department of Chemistry, Razi University, Kermanshah, Iran.*

E -mail:mshamsipur@yahoo.com

[b] *Dipartimento di Scienze Chimiche e Geologiche, Universita` degli Studi di Cagliari, S.S. 554 Bivio per Sestu, 09042 Monserrato CA, Italy*

Introduction

Uranium is highly radioactive and is extensively used in the nuclear industry, and is well known as a chemical toxin.[1] In nature, hexavalent uranium is commonly associated with oxygen in the uranyl ion, UO_2^{2+}. The UO_2^{2+} is among those ions for which a search for a suitable sensor continues owing to its importance in various geochemical, physiological, medical and industrial processes.[2,3] It is present in low quantities (10^{-5} to 10^{-3} M) in wash streams coming out from nuclear reactors both in aqueous and nonaqueous media and, as such, constant monitoring of these streams for the presence of uranium in high activity content is essential.[3]

Many methods have been developed for the determination of uranium, based on different techniques, such as ion selective electrodes,[4,5] nuclear techniques,[6] inductively coupled plasma-mass spectrometry,[7,8] electrochemistry,[9-11] fluorimetry[12,13] and spectrophotometry.[14-16] These methods are either time consuming, involving multiple sample manipulations or too expensive for most analytical laboratories. It is worth mentioning that the development of optical sensors has now become a rapidly expanding area of analytical chemistry, because they offer the advantages of simple preparation, reasonable selectivity and sensitivity and no need for separate reference devices.[17-21] Compared to ion-selective electrodes, optical sensors based on absorbance or fluorescence have additional feature possibilities in that they may take advantage of spectral properties associated with the analyte or analyte specific indicator.[17,22,23] Fluorescence is particularly a suitable optical sensing method for designing these optical sensors. This is mainly due to its inherent sensitivity, almost complete inertness to turbidity and flexibility with respect to geometric arrangements.[17]

In the past two decades, much work has been directed to the development of fluorescent sensors for different metal ions, which offer distinct advantages in terms of sensitivity, selectivity, response time and remote control.[24-28] The theoretical basis of such optical membranes based on plasticized PVC has also been well established.[24,29,30] In developing such fluorescent ionic sensors, in addition to high selectivity towards the ion of interest, a large change in fluorescence intensity in the presence of the ion and/or a spectral change is required to ensure the sensitivity of the sensing process.[22,23] Thus, in the case of such fluorescence sensors, the key point is the design of a fluorescence sensing element which usually consists of a fluorophore (signaling moiety) linked to an ionophore (recognition moiety), called as fluoroionophore.[31,32] The recognition process by fluoroionophores takes place by their ionophore part which is then converted to a change in the fluorophore's signal, brought about by the perturbation of such photoinduced processes as energy transfer, charge transfer, electron transfer, formation or disappearance of eximers and exciplexes.[26,31,32] In most of the reported sensing systems, the metal ions quench the fluorescence via different mechanisms.[32,34] However, there are only few examples in which the complexation of cations result in fluorescence enhancement (usually called as metal-induced fluorescence).[35-37]

In the present study the suitability of 5-(9-anthracenylmethyl)-5-aza-2,8-dithia[9],(2,9)-1,10-phenanthrolinophane (**L**) (Fig. 1) for the preparation of uranyl PVC optical membrane sensor has been investigated and utilized for the determination of uranyl ion concentration in water samples with satisfactory results.

(Fig. 1)

Experimental

Reagents and apparatus

All of the chemicals were used of analytical reagent grade (Merck). Doubly distilled water was used throughout. Dibutylphthalate (DBP), dioctylphthalate (DOP), tris(2-ethylhexyl)phosphate (TEHP), dioctylsebasate (DOS), tetrahydrofuran (THF), sodium tetraphenylborate (NaTPB) and high relative molecular weight poly(vinyl chloride) (PVC) were obtained from Merck or Sigma and used without any further purification. 2-Nitrophenyloctylether (NPOE) was purchased from Acros. The 5-(9-anthracenylmethyl)-5-aza-2,8-dithia[9],(2,9)-1,10-phenanthrolinophane (**L**) was synthesized and its structure has been approved, as reported before.[38] Also, the nitrate salts of all cations used (all from Merck) were of the highest purity available and were used without any further purification.

All fluorescence measurements were carried out on a Varian Cary Eclipse fluorescence spectrometer. A Metrohm 692 pH/ion meter was used for the pH measurements.

Optode preparation

PVC-based uranyl membrane sensors were prepared by thoroughly mixing 7 mg of fluoroionophore **L**, 2 mg of additive (NaTPB), 31 mg of powdered PVC and 60 mg of plasticizer NPOE in a glass dish of 2 cm diameter. The mixture was then completely dissolved in 2 mL of fresh THF. Glass plates (28 mm × 28 mm with 1 mm thickness) were cut into 28 mm × 13 mm pieces to fit easily into a quartz cell (10 mm × 10 mm × 50 mm). The plates were cleaned with THF. Then, they were rinsed with water and finally dried in an oven at 110 °C. The membranes were cast by placing 0.2 mL of the homogenized membrane solution onto the glass slide, and spread quickly using spin-on device (2600 rpm rotation frequency). After a spinning time of about 15 s, the glass support plate with sensing membrane was removed and allowed to stand in ambient air for 1 h before use. As is quite usual in the case of optode membrane systems [32,34], in this work, the membrane thickness (T) was estimated from calculations based on the coated membrane area (A = 28 mm × 13 mm) and volume (V) and density (D) of the membrane solution introduced and uniformly spread on the glass plates. The thickness of dry membrane thus obtained found to be approximately (400 ± 25) μm. The polymer films were placed in diagonal position in the cell containing 2.0 mL acetate buffer solution of pH 4.0, and a membrane (without fluoroionophore) at the same conditions was used as a blank membrane. The film was first soaked for more than 20 min until the membrane revealed a stable fluorescence value before the first uranyl ion measurement was made. During titration, the fluorescence intensity at an excitation wavelength of 366 nm was measured at 425 nm. Then the sample was titrated with standardized uranyl ion solutions and the fluorescence intensity of the system was measured after ∼3 min, required to reach the equilibrium.

Water solubility and partition coefficient of L

The water solubility of **L** was examined as follows. Milligram amounts of **L** were shaken with 50.0 mL of water overnight at 25 °C. Then the mixture was centrifuged, and the remaining ligand was weighed after vacuum drying.

The experimental procedure for obtaining the partition coefficient of **L** was as follows. A 20.0 mL portion of 1-octanol solution containing 1.0 mg of **L** and an equal volume of water were introduced to a stoppered glass tube (volume of 50.0 mL) and was shaken in a thermostated water bath at 25 °C overnight. The **L** concentration in organic phase was then measured spectrophotometrically at 370 nm after separation of the two phases. The partition coefficient was then determined using the equilibrium concentrations of **L** in water and 1-octanol.

Results and discussion

5-(9-anthracenylmethyl)-5-aza-2,8-dithia[9],(2,9)-1,10-phenanthrolinophane (**L**) with phenanthroline and anthracene groups in its structure and negligible water solubility was expected to act as a suitable ionophore in the preparation of PVC membrane sensors for given transitional and heavy metal ions of proper size and charge. It should be noted that the solubility of **L**, obtained by shaking an excess of ligand with water overnight at 25 °C and developing the results gravimetrically, was found to be $(1.1\pm0.2) \times 10^{-4}$ M. Moreover, the partition coefficient of L between water and 1-octanol was determined by using various ligand concentrations in equal phase volumes and equilibrating for 12 h. The equilibrium concentrations of **L** in both phases were determined spectrophotometrically, as described in the Experimental section. The resulting partition coefficient value was $K = [L]_{aq}/[L]_{org} = (4.02\pm0.05) \times 10^{-3}$, which is quite suitable for its use as ionophore in the PVC membrane sensors with negligible leakage from the membrane phase into aqueous solutions.[24]

Preliminary studies

Similarly to other anthracenylmethyl derivatives of azamacrocycles used as fluorescence chemosensors for different metal ions,[26,39-42] a 5.00×10^{-5} M solution of **L** in acetonitrile showed the typical fluorescence emission spectrum of the anthracene fragment at the excitation wavelength of 370 nm, having a maximum intensity at 421 nm (Fig. 2). The addition of uranyl ion to the solution of **L** in acetonitrile results in a pronounced chelation enhancement of fluorescence (CHEF effect),[43] while both the shape and position of the fluorescence emission spectrum remain unchanged. Such behavior is typical for anthracenylmethyl derivatives of azamacrocycles in the presence of metal ions, and it is a direct consequence of the coordination of the tertiary N-donor to the metal ion that reduces the photoinduced electron transfer (PET) from the lone pair on this nitrogen to the anthracene moiety in the excited state.[26,39-42]

(Fig. 2)

The fluorescence intensity versus M^{n+}/**L** molar ratio plots for the case of UO_2^{2+} ion and some potential interfering metal cations such as Al^{3+}, La^{3+}, Ce^{3+}, Pr^{3+}, Sm^{3+}, Ag^{+}, Cd^{2+}, Hg^{2+} and Pb^{2+} are shown in Fig. 3. For all cations examined, the observed CHEF effect tends to level off at a M^{n+}/**L** molar ratio of 0.5, indicating the formation of 2:1 **L**/M^{n+} complexes in acetonitrile solution. The formation constants of the resulting complexes were evaluated by fitting the fluorescence intensity-metal ion molar ratio data using a nonlinear least squares curve-fitting program, as described elsewhere.[44] The results are summarized in Table 1. It is interesting to note that the CHEF effect observed for **L** in the presence of different metal cations decreases in the order $UO_2^{2+} > Al^{3+} > La^{3+} > Ce^{3+} > Pr^{3+} > Sm^{3+} > Ag^{+} > Cd^{2+} > Hg^{2+} > Pb^{2+}$, which presumably reflects the order of formation constants of the corresponding $[M(\mathbf{L})_2]^{n+}$ complexes and, consequently, the selectivity order of **L** for these different cations.

(Fig. 3) and (Table 1)

To obtain more information about the conformational changes of **L** upon complexation to the uranyl ion, the molecular structures of the free ligand and its 2:1 complex with UO_2^{2+} were optimized using the DFT-B3LYP/6-31G* method.[45] The DFT-B3LYP/6-31G* calculations showed for different stable forms (Fig. 4A, conformers 1-4) with different point groups, among which the conformer-1 with a point group of C_S is the most stable form with 4.78, 6.88 and 10.37 kcal mol^{-1} higher energies than the conformers 2, 3 and 4, respectively. In fact the conformer-1 possesses the largest cavity area and volume among different forms calculated.

The uranyl ion ($[UO_2]^{2+}$) is an oxycation of uranium in the oxidation state +6. It has a linear and symmetrical structure (with point group $D_{\infty h}$) possessing short U-O bonds of 1.80 Å, indicative of the presence of multiple bonds between uranium and oxygen. The most common arrangement reported for uranyl ion complexes is a distorted octahedral structure, in which the so-called equatorial ligands are lied in a plane perpendicular to the O-U-O line and passing through the uranium atom.[46]

Molecular mechanics is presently the only practical method for calculations on very large molecules or for conformational searching on highly flexible molecules. The Merck Molecular Force Field method (MMFF94), in particular, has proven to be a reliable and fast tool for conformational and structural analysis. There are no atom limits for molecular mechanics calculations. There is in fact no Hamiltonian available to calculate the structures of uranyl ion complexes by SCF-MO, DFT and ab-initio quantum mechanical methods. Thus, in this work, we employed the molecular mechanics-MM (MMFF94) method for the structural calculation of the $[UO_2(\mathbf{L})_2]^{2+}$ complex. Fig. 4B shows the three possible structures (structures 1-3), with different point groups, for the complex calculated by the MMFF94 method. The calculation results clearly revealed that the structure-1 (point group C_{2h}) is more stable than structure-2 (point group C_2) and structure-3 (point group C_i) by 3.45 and 22.95 kcal mol^{-1}, respectively. The bond angles of O-U-O in $[UO_2]^{2+}$ for the most stable complex was obtained as 180°. The calculated results by the MMFF94 method showed that the amino nitrogen and two sulfur atoms of the cavities of the two ligands participate in binding with central uranyl ion, while there is no binding from the phenanthroline nitrogens of the ligand.

(Fig. 4)

The conformation having the lowest energy content calculated for the free ligand (Fig. 4A) shows that the phenanthroline moiety and the anthracenyl group are well separated from each other, with the latter pointing away from the macrocyclic cavity. This conformation may possibly facilitate the photoinduced electron transfer (PET) from the amino group to the anthracene group, thus affording a relatively weakly fluorescent system.[32-35] However, in the optimized structure of the complex $[UO_2(\mathbf{L})_2]^{2+}$ (Fig. 4B), the uranyl ion coordinates to the amino nitrogens and the sulfur donor atoms of the two ligand molecules, and forces the phenanthroline and anthracene fragments of each ligand unit to get closer in an almost stacked disposition, although no significant interactions between them are found. Furthermore, in the complex, the macrocyclic moieties of **L** assumes a folded conformation with the aliphatic portion tilted over the phenanthroline fragment as normally found in macrocycles containing a phenanthroline subunit.[36] Therefore, the formation of the complex $[UO_2(\mathbf{L})_2]^{2+}$ not only prohibits to large extent the electron transfer from the tertiary amino group to the fluorogenic moiety of the two ligand units, but also significantly reduces the flexibility of the ligand. In this case, due to the occurrence of the CHEF effect, the resulting complex is expectedly shows a sharp increase in its fluorescence.[47]

According to these preliminary results and considering the high lipophilic character of the complex $[UO_2(\mathbf{L})_2]^{2+}$, we expected the ligand **L** to act as a suitable ionophore for uranyl ion in a PVC membrane optode.

Operation principle

The proposed membrane sensor was prepared by incorporation of the lipophilic fluoroionophore **L** in plasticized PVC containing NaTPB as a lipophilic anionic additive. The fluoroionophore possesses unique binding properties to uranyl ions and its fluorescence is strongly and selectively enhanced as a result of the binding event. The lipophilic anionic sites, TPB^-, provide the optode membrane with the necessary ion-exchange properties, because the fluoroionophore acts as a neutral ligand and, therefore, cannot function as an ion exchanger. Under the experimental conditions used and considering the formation of a 2:1 $\mathbf{L}/UO_2^{2+}$ complex in the organic phase, the response mechanism of the proposed optical system can be explained by the following ion-exchange pathway:[22,48,49]

$$UO_2^{2+}{}_{(aq)} + 2\,\mathbf{L}_{(org)} + 3NaTPB_{(org)} = [UO_2^{2+}(\mathbf{L})_2]^{2+}{}_{(org)} + 3TPB^{-}{}_{(org)} + 3Na^{+}{}_{(aq)} \qquad (1)$$

The fluorescence excitation and emission spectra of the fluorescent optode membrane in an acetate buffer solution of pH 4.0 and in the presence of increasing concentrations of uranyl ion are shown in Fig. 5. As it is quite obvious, both the excitation and emission intensities are increased upon increasing concentration of uranyl ion in the buffer solution at pH 4. Based on the response mechanism of the optical sensor, the theoretical principle of the optode membrane determination is proposed as follows. If the equilibrium between uranyl ion in the aqueous solution $M_{(aq)}$ and L in the plasticized PVC membrane phase $L_{(org)}$ form a M_mL_n complex, the overall equilibrium can be represented as follows:

$$mM_{(aq)} + n\,\mathbf{L}_{(org)} = M_m\,\mathbf{L}_{n(org)} \qquad (2)$$

$$K = [M_m\mathbf{L}_n]_{org} \;/\; [M]^{m}_{aq}\,[\mathbf{L}]^{n}_{org} \qquad (3)$$

where *m* and *n* designate the complexing ratio between uranyl ions and L, and K is the equilibrium constant of the overall reaction. By definition, the relative fluorescence intensity, is the ratio of uncomplexed **L** in the membrane phase, $[\mathbf{L}]_{org}$ to its total amount, $[\mathbf{L}_t]_{org}$ so that:

$$\alpha = [\mathbf{L}]_{org} / [\mathbf{L}_t]_{org} \quad \text{and} \quad [M_m\,\mathbf{L}_n]_{org} = [\mathbf{L}_t]_{org}\,(1-\alpha)/n \qquad (4)$$

In practice, the α value can be determined by measuring the fluorescence intensity of the optical sensor, FI during titration with uranyl ions:

$$\alpha = (FI - FI_0) / (FI_t - FI_0) \qquad (5)$$

where FI_0 and FI_t are the limiting fluorescence intensities of the optical sensor at α = 0 (i.e., uncomplexed **L**) and α = 1 (i.e., totally complexed **L**), respectively. Thus, the relationship between the α-value and the concentration of uranyl ion in aqueous sample solution, $[M]_{aq}$ can be obtained by combining Eqs. (3) and (4), as follows:

$$(1 - \alpha)/\ \alpha^{n} = nK[\mathbf{L}_{t}]^{n-1}{}_{org}[M]^{m}{}_{aq} \qquad (6)$$

Eq. (6) can then be used as a basis for the quantitative determination of uranyl ions, using the proposed optical membrane.

(Fig. 5)

Effect of membrane composition

It is well known that the membrane composition may largely influence the response characteristics and working concentration ranges of the optical sensors.[22,23,25] In order to choose the best composition of the membrane solution used in membrane preparation, the influences of the fluoroionophore and NaTPB concentrations and the plasticizer type on the response range of the optical sensor withrespect to uranyl ion were examined. The results of this study are summarized in Table 2. It is noteworthy that the best membrane characteristics is reported to usually obtain at a plasticizer/PVC ratio of 1.6–2.2.[32,50]

In addition, the nature of plasticizer is well-known to influence largely the measuring concentration rang of the solvent polymeric sensors as well as their selectivity coefficients.[50,51] As it is immediately obvious from Table 2, under the optimal membrane composition, the use of NPOE as plasticizer resulted in a large widening of the measuring range of the proposed optical sensor. In bulk liquid membrane optodes, a mass transfer of analyte from the sample solution into the membrane is required, in order to facilitate the establishment of a thermodynamic equilibrium between the membrane and the sample.[51,52] Thus, in the proposed uranyl-selective membrane sensor containing **L** as a neutral fluoroionophore, the presence of a lipophilic anionic additive like NaTPB was found to be necessary to facilitate the corresponding ion-exchange equilibrium.

Table 2 shows that the presence of 7 mg of fluoroionophore **L** in membrane resulted in the best response of the Uranyl selective sensor. Thus, the membrane number 1 with an optimized PVC:NPOE:NaTPB:**L** wt% ratio 31:60:2:7 was used for further studies.

(Table 2)

Effect of pH on the sensor response

The effect of pH of test solution on the fluorescence response of the proposed sensor was tested in the pH range of 2–6. The fluorescence intensity measurements were made for 1.0 × 10^{-6} M uranyl ion at different pH values. The pH of solution was adjusted by either NaOH or HNO_3. As it is seen from Fig. 6, the fluorescence intensity increases with increasing pH of solution and reaches a maximum value at a pH 4.0, and then decreases. The decreased intensity at lower pH might be due to the extraction of H^+ from the aqueous sample solution into the PVC-membrane, via **L** molecule, leading to an expected change in the mobility of electrons of the system. On the other hand, the reduced optical response at pH > 4.0 could be due to a possible slight swelling of the polymeric film under alkaline conditions, as well as the hydroxide formation of uranyl ions, resulting in decreased concentration of free uranyl ions in sample solution. Thus, in subsequent experiments, a solution of pH 4.0, adjusted by acetate buffer, was used for further studies.

(Fig. 6)

Response time and regeneration

The dynamic response time, as an important characteristic of any ion-selective membrane sensor, was studied in this work. The results revealed that all response times for reaching equilibrium between the sensing membrane and the analyte and giving a steady-state fluorescence signal found to be about 3 min, after changing the uranyl ion concentration from 10^{-9} to 10^{-3} M in a stepwise manner. The fluorescence signal of the optode membrane was not completely recovered when the solution was switched from high-to-low uranyl ion concentrations. Such irreversibility is obviously a drawback for the sensor device. However, after immersion of a used optical membrane for one minute in a 0.01 M EDTA, the fluorescence was found to be fully recovered. The regeneration of **L** present in the optode membrane can be afforded by complete stripping of uranyl ion from the membrane, as it was confirmed by getting back to the original fluorescence intensity.

Dynamic range and detection limit

The optical response of the proposed uranylselective sensor at different uranyl ion concentrations, under optimal experimental conditions, is shown in Fig. 7. Three curves are calculated using Eq. (6) with different m: n ratios. As it seen the curve with 1:2 uranyl-**L** stoichiometric complex ratio and an appropriate K value of 5×10^6 fits best to the experimental data. In fact, the mechanism of the response of optode is believed to be based on complexation of **L** and uranyl. This curve can be suitably used as a calibration curve for the determination of uranyl ions in a concentration range of 1.0×10^{-10} to 1.0×10^{-3} M. The LOD and LOQ estimated as the concentration of analyte producing an analytical signal equal to three and ten times of the standard deviation of the blank signal (evaluated as 0.9×10^{-11}) respectively, were 2.7×10^{-11} M and 9.0×10^{-11} M.

(Fig. 7)

Short-term stability, repeatability, and life time

To study the short-term stability of the optode membrane, its fluorescence intensity in contact with 1.0×10^{-6} M solution of uranyl buffered at pH 4.0 was recorded over period of 2 h. From the fluorescence intensities taken every 15 min, it was found that there was no evidence of leakage of **L** from the membrane during this period. The repeatability of the sensor membrane was evaluated by measuring uranyl concentration with a single sensor (n=5). The relative standard deviations (RSD) of 2.0% and 2.1%, were obtained for 1.0×10^{-6} and 1.0×10^{-8} M uranyl, respectively. The reproducibility was examined by preparing five different membranes with the same composition, and measuring the fluorescence intensity of each membrane in a 1.0 × 10^{-6} M uranyl (five repeated determinations) in acetate buffer solutions of pH 4.0. The resulting coefficient of variation was found to be ±2.5%. The optode was stable over a period of 3 months when not in use (membrane was kept in air) and the signal value of the membrane did not change.

Selectivity

The optical membrane selectivity, which reflects the response of the sensor for primary ion over diverse ions present in solution, is perhaps the most important characteristics of an ion selective optode. Thus, the influence of a number of common metal ions on the fluorescence intensity of uranyl sensor was investigated. The experiments were carried out by fixing the concentration of uranyl at 1.0 × 10^{-6} M and then recording the change in fluorescence intensity before (F_0) and after adding the interfering ion at a 1.0 × 10^{-4} M level (F) into the uranyl solution buffered at pH 4. The results of selectivity studies are summarized in Fig. 8. As can be seen, the relative error of several interfering ions is less than ±4%, which is recognized as tolerated. As it is obvious, the proposed optical sensor possesses good selectivity for uranyl, so that the disturbance produced by the other cations tested in the functioning of the proposed uranyl optical sensor is negligible.

(Fig. 8)

Analytical applications

In order to investigate the potential use of the developed optical sensor for the determination of uranyl, it was applied to samples of tap water. Tap water samples were used without a previous treatment, and known amounts of uranyl were spiked with standard stock solution and determined by the proposed optical membrane. Results are shown in Table 3. The results show that the sensor is suitable for determination of uranyl concentrations with a good precision and accuracy. As it can be seen, all calculated t-values at 95% confidence level are well below the tabulated value of 2.31.

(Table 3)

The proposed system was also applied to the determination of uranyl content of a spring water sample near the Khoshomi uranium mines (Yazd, Iran). The concentration of uranyl ion obtained from triplicate measurements with fluorescent sensor (62.0 ± 0.6 ppm) was found to be in satisfactory agreement with that determined by ICP-AES (62.4 ± 0.3 ppm). The satisfactory results of the corresponding recovery tests are also added in Table 4.

(Table 4)

Furthermore, the selectivity and applicability of the proposed sensor was also tested by the determination of the uranyl content in two mixtures of containing excess amounts of potential interfering ions and the results are summarized in Table 5. The results thus obtained clearly indicated that the new optical sensor acts quite selective, precise and accurate. Moreover, both calculated t-values at 95% confidence level are well below the tabulated value of 2.31.

(Table 5)

Comparison with previous optical sensors for uranium ion

In Table 4, the main analytical characteristics (i.e., response time, dynamic range, pH and detection limit) of the proposed fluorescent sensor were compared with the recent reported uranyl optodes.[14,53-59] As it can be seen from the data summarized in Table 4, the proposed sensor is significantly improved compared to the previously reported uranyl sensors in terms of response time, dynamic range and detection limit. Moreover, due to its highly selective behavior, the proposed fluorescence sensor is applicable to the accurate determination of the uranyl ion in real samples of complex matrices, as shown in the section of analytical applications.

(Table 4)

Conclusions

In this work, an efficient and selective fluorimetric optode membrane for uranyl ion detection at low concentration levels is described. It is based on the enhancement of the fluorescence emission of 5-(9-anthracenylmethyl)-5-aza-2,8-dithia[9],(2,9)-1,10-phenanthrolinophane (**L**) at 425 nm (λ_{ex} = 366 nm), upon selective complexation with uranyl ions. It is fully reversible and can be easily regenerated from high concentration to low concentration. The proposed sensor revealed exellent response characteristics with respect to stability, reproducibility, calibration range, detection limit and selectivity, so that it can be ranked among the best optical chemical sensors reported for uranyl ion. The performance characteristics of the proposed sensor, including its high selectivity and low detection limit, can tentatively be explained in terms of the high formation constant of the 1:2 complex between uranyl ion and **L**, as measured in the organic phase. The proposed fluorescent sensor was successfully applied to the direct determination of uranyl content in aqueous solutions and, especially, in a spring water sample near the Khoshomi uranium mines (Yazd, Iran).

Acknowledgements

The support of this work by the Iran National Elite Foundation (INEF) is gratefully acknowledged.

References

1 R. Lewis Sr, 25. Sax’s Dangerous Properties of Industrial Materials, John Wiley & Sons Inc., New York, 2000.
2 M. Shamsipur, A. R. Ghiasvand and Y. Yamini, Solid-phase extraction of ultratrace uranium(VI) in natural waters using octadecyl silica membrane disks modified by tri-

n-octylphosphine oxide and its spectrophotometric determination with dibenzoylmethane, *Anal. Chem.*, 1999, **71**, 4892-4895.

3 S. Y. Bae, G. L. Southard and G. M. Murray, Molecularly imprinted ion exchange resin for purification, preconcentration and determination of UO_2^{2+} by spectrophotometry and plasma spectrometry, *Anal.Chim. Acta*, 1999, **397**, 173-181.

4 M. R.Ganjali, Z. Memari, R. Dinarvand, F. Faridbod and P. Norouzi, Uranyl plasticized membrane sensor based on a new calix[4]arene, *Sens. Lett.*, 2009, **7**, 1156-1162.

5 R. Ansari and Z. Mosayebzadeh, Construction of a new solid-state U(VI) ion-selective electrode based on polypyrrole conducting polymer, *J. Radioanal. Nucl. Chem.*, 2014. **299**, 1597-1605.

6 M. Blanco Rodríguez, F. Vera Tomé, J. Lozano and V. Gómez Escobar, Sequential method for the determination of uranium, thorium and ^{226}Ra by liquid scintillation alpha spectrometry, *Appl. Rad. Isotopes*, 2000, **52**, 705-710.

7 Y. Zheng, B. Weinman, T. Cronin, M. Fleisher and R. Anderson, A rapid procedure for the determination of thorium, uranium, cadmium and molybdenum in small sediment samples by inductively coupled plasma-mass spectrometry: application in Chesapeake Bay, *Appl. Geochem., 2003*,**18**, 539-549.

8 F. A. Aydin and M. Soylak, Solid phase extraction and preconcentration of uranium (VI) and thorium (IV) on Duolite XAD761 prior to their inductively coupled plasma mass spectrometric determination, *Talanta*, 2007, **72**, 187-192.

9 M. Jarczewska, R. Ziółkowski, Ł. Górski and E. Malinowska, Electrochemical uranyl cation biosensor with DNA oligonucleotides as receptor layer, *Bioelectrochem.*, 2014, **96**, 1-6.

10 L. Zhang, C.-Z. Wang, H.-B. Tang, L. Wang, Y.-S. Liu, Y.-L. Zhao, Z.-F. Chai and W.-Q. Shi, Rapid determination of uranium in water samples by adsorptive cathodic stripping voltammetry using a tin-bismuth alloy electrode, *Electrochim. Acta*, 2015, **174**, 925–932.

11 Y. Peled, E. Krent, N. Tal, H. Tobias and D. Mandler, Electrochemical determination of low levels of uranyl by a vibrating gold microelectrode, *Anal. Chem.*, 2015, **87**, 768–776.

12 S. S. Hosseiny Davarani, H. R. Moazami, A. R. Keshtkar, M. H. Banitaba and S. Nojavan, A selective electromembrane extraction of uranium (VI) prior to its fluorometric determination in water, *Anal. Chim. Acta*, 2013, **783**, 74–79.

13 X. Chen, L. He, Y. Wang, B. Liu and Y. Ta Trace, analysis of uranyl ion (UO_2^{2+}) in aqueous solution by fluorescence turn-on detection via aggregation induced emission enhancement effect, *Anal. Chim. Acta*, 2014, **847**, 17, 55–60.

14 M. Shamsipur, K. Zargoosh, F. Mizani, H. Eshghi and F. Rostami, A novel PVC-membrane optical sensor for highly sensitive and selective determination of UO_2^{2+} ion based on a recently synthesized benzo-substituted macrocyclic diamide and dibenzoylmethane, *Spectrochim. Acta A*, 2010, **77**, 319–323

15 T. Madrakian, A. Afkhami and M. Rahimi, Removal, preconcentration and spectrophotometric determination of U(VI) from water samples using modified maghemite nanoparticles, *J. Radioanal. Nucl. Chem.*, 2012, **292**, 597-602.

16 N. Drogat, L. Jauberty, V. Chaleix, R. Granet, E. Guénin,V. Sol and V. Gloaguen, Sensing of the uranyl ion based on its complexation with bisphosphonate-capped gold nanoparticles, *Mater. Lett.*, 2014, **122**, 208–211.

17 J. R. Lakowicz, Topics in Fluorescence Spectroscopy; Volume 4, Probe Design and Chemical Sensing, Springer, 1994.

18 H. Hisamoto and K. Suzuki, Ion-selective optodes: current developments and future prospects, *TrAC Trends Anal. Chem.*, 1999, **18**, 513-524.

19 O. S. Wolfbeis, Fiber-optic chemical sensors and biosensors, *Anal. Chem.*, 2000, **72**, 81R-90R.

20 X. Yuan, Z. Luo, Y. Yu, Q. Yao and J. Xie, Luminescent noble metal nanoclusters as an emerging optical probe for sensor development, *Chem. Asian J.*, 2013, **8**, 858–871.

21 J. R. Askim, M. Mahmoudi and K. S. Suslick, Optical sensor arrays for chemical sensing: the optoelectronic nose, *Chem. Soc. Rev.*, 2013, *42*, 8649-8682.

22 E. Bakker, P. Bühlmann and E. Pretsch, Carrier-based ion-selective electrodes and bulk optodes. 1. General characteristics, *Chem. Rev.*, 1997, **97**, 3083-3132.

23 J. P. Desvergne and A. W. Czarnik, Chemosensors of Ion and Molecule Recognition, Springer, N.Y., 1997.

24 P. Bühlmann, E. Pretsch and E. Bakker, Carrier-based ion-selective electrodes and bulk optodes. 2. Ionophores for potentiometric and optical sensors, *Chem. Rev.*, 1998, **98**, 1593-1688.

25 A. P. de Silva, H. Q. N. Gunaratne, T. Gunnlaugsson, A. J. M. Huxley, C. P. McCoy, J. T. Rademacher and T. E. Rice, Signaling recognition events with fluorescent sensors and switches, *Chem. Rev.*, 1997, **97**, 1515-1566.

26 B. Valeur and I. Leray, Design principles of fluorescent molecular sensors for cation recognition, *Coord. Chem. Rev.*, 2000, **205**, 3-40.

27 M. Formica, V. Fusi, L. Giorgi and M. Micheloni, New fluorescent chemosensors for metal ions in solution, *Coord. Chem. Rev.* 2012, **256**, 170–192.

28 K. P. Carter, A. M. Young and A. E. Palmer, Fluorescent sensors for measuring metal ions in living systems, *Chem. Rev.*, 2014, **114**, 4564–4601.

29 R. Eugster, U. E. Spichiger and W. Simon, Membrane model for neutral-carrier-based membrane electrodes containing ionic sites, *Anal. Chem.*, 1993, **65**, 689-695.

30 W. E. Morf, K. Seiler, B. Lehmann, C. Behringer, K. Hartman and W. Simon, Carriers for chemical sensors: Design features of optical sensors (optodes) based on selective chromoionophores, *Pure Appl. Chem.*, 1989, **61**, 1613-1618.

31 M. C. Aragoni, M. Arca, A. Bencini, A. J. Blake, C. Caltagirone, G. De Filippo, F. A. Devillanova, A. Garau, T. Gelbrich, M. B. Hursthouse, Tuning the selectivity/specificity of fluorescent metal ion sensors based on N2S2 pyridine-containing macrocyclic ligands by changing the fluorogenic subunit: spectrofluorimetric and metal ion binding studies, *Inorg. Chem.*, 2007, **46**, 4548-4559.

32 M. Shamsipur, K. Alizadeh, M. Hosseini, C. Caltagirone and V. Lippolis, A selective optode membrane for silver ion based on fluorescence quenching of the dansylamidopropyl pendant arm derivative of 1-aza-4,7,10-trithiacyclododecane ([12]aneNS3), *Sens. Actuators B*, 2006, **113**, 892-899.

33 E. U. Akkaya, M. E. Huston and A. W. Czarnik, Chelation-enhanced fluorescence of anthrylazamacrocycle conjugate probes in aqueous solution, *J. Am. Chem. Soc.*, 1990, **112** 3590-3593.

34 M. Shamsipur, M. Sadeghi, K. Alizadeh, H. Sharghi and R. Khalifeh, An efficient and selective flourescent optode membranebased on 7-[(5-chloro-8-hydroxy-7-quinolinyl)methyl]-5,6,7,8,9,10-hexahydro-2H-1,13,4,7,10-benzodioxatriazacyclopentadecine-3,11(4H,12H)-dione as anovel fluoroionophore for determination of cobalt(II) ions, *Anal. Chim. Acta*, 2008, **630**, 57-66.

35 P. Ghosh, P. K. Bharadwaj, J. Roy and S. Ghosh, Transition metal (II)/(III), Eu (III), and Tb (III) ions induced molecular photonic OR gates using trianthryl cryptands of varying cavity dimension, *J. Am. Chemi. Soc.*, 1997, **119**, 11903-11909.

36 B. Ramachandram and A. Samanta, Modulation of metal–fluorophore communication to develop structurally simple fluorescent sensors for transition metal ions, *Chem. Commun.*, 1997, 1037-1038.

37 H. Sakamoto, J. Ishikawa, S. Nakao and H. Wada, Excellent mercury (II) ion selective fluoroionophore based on a 3, 6, 12, 15-tetrathia-9-azaheptadecane derivative bearing a nitrobenzoxadiazolyl moiety, *Chem. Commun.*, 2000, 2395-2396.

38 M. Shamsipur, F. Mizani, K. Alizadeh, M. F. Mousavi, V. Lippolis, A. Garau and C. Caltagirone, Flow injection potentiometry by a novel coated graphite electrode based on 5-(9-anthracenylmethyl)-5-aza-2, 8-dithia [9],(2, 9)-1, 10-phenanthrolinophane for the selective determination of uranyl ions, *Sens. Actuators B*, 2008, **130**, 300-309.

39 A. J. Blake, A. Bencini, C. Caltagirone, G. De Filippo, L. S. Dolci, A. Garau, F. Isaia, V. Lippolis, P. Mariani and L. Prodi, A new pyridine-based 12-membered macrocycle functionalised with different fluorescent subunits; coordination chemistry towards CuII, ZnII, CdII, HgII, and PbII, *Dalton Tran.*, 2004, 2771-2779.

40 A. Tamayo, C. Lodeiro, L. Escriche, J. Casabó, B. Covelo and P. González, New fluorescence PET systems based on N2S2 pyridine-anthracene-containing macrocyclic ligands. Spectrophotometric, spectrofluorimetric, and metal ion binding studies, *Inorg. Chem.*, 2005, **44**, 8105-8115.

41 P. A. de Silva, N. H. Q. Gunaratne and C. P. McCoy, A molecular photoionic and gate based on fluorescent signalling, *Nature*, 1993, **364**, 42-44.

42 E. Kimura and T. Koike, Recent development of zinc-fluorophores, *Chem. Soc. Rev.*, 1998, **27**, 179-184.

43 J. R. Lakowicz and C. D. Geddes, Topics in fluorescence spectroscopy, Springer, N.Y., 1991.

44 J. Ghasemi and M. Shamsipur, Spectrophotometric study of the thermodynamics of interaction of some metal ions with murexide in binary acetonitrile-dimethylsulfoxide mixtures, *J. Coord. Chem.*, 1995, **36**, 183-194.

45 All of the calculations were performed by: Spatran ’10-Quantum Mechanics Program: (PC/x86) 1.1.0v4. 2011, Wavefunction Inc., USA.

46 S. Cotton, Lanthanides and Actinides, Oxford University Press, New York, 1991.

47 J. R. Lakowicz, C. D. Geddes, Topics in Fluorescence Spectroscopy, Springer, New York, 1991.

48 M. Shamsipur, M. Mohammadi, A. (A.) Taherpour, V. Lippolis and R. Montis, Development of a novel PVC-membrane fluorescent sensor based onN,N’-bis(dansylamidoethyl)-N,N’-bis(2-pyridylmethyl)propylene-diamine as a new fluoroionophore for highly sensitive and selectivemonitoring of trace amounts of La^{3+} ions in aqueous solutions, *Sens. Actuators B,* 2014, **192**, 378–385.

49 M. Shamsipur, M. Sadeghi, M. H. Beyzavi and H. Sharghi, Development of a novel fluorimetric bulk optode membrane based on meso-tetrakis(2-hydroxynaphthyl) porphyrin (MTHNP) for highly sensitive and selective monitoring of trace amounts of Hg^{2+} ions, *Mater. Sci. Eng. C*, 2015, **48**, 424–433.

50 N. Ertaş, E. U. Akkaya and O. Yavuz Ataman, Simultaneous determination of cadmium and zinc using a fiber optic device and fluorescence spectrometry, *Talanta*, 2000, 51, 693-699.

51 T. Rosatzin, E. Bakker, K. Suzuki and W. Simon, Lipophilic and immobilized anionic additives in solvent polymeric membranes of cation-selective chemical sensors, *Anal. Chim. Acta*, 1993, 280, 197-208.

52 A. K. Singh, R. Singh and P. Saxena, Cobalt (II)-selective electrode based on a newly synthesized macrocyclic compound, *Sens. Actuators B,* 2006, **114**, 578-583.

53 A. Safavi, M. Bagheri, A novel optical sensor for uranium determination, *Anal. Chim. Acta*, 2005, **530**, 55-60.

54 S. Sadeghi, S. Doosti, Novel PVC membrane bulk optical sensor for determination of uranyl ion, *Sens. Actuators B,* 2008, **135**, 139-144.

55 V. Zare-Shahabadi, M. Akhond, J. Tashkhourian and F. Abbasitabar, Characterization of a new uranyl selective bulk optode; utilizing synergistic effect in optical sensor, *Sens. Actuators B*, 2009, **141**, 34-39.

56 M. Ghaedi, J. Tashkhourian, M. Montazerozohori, A. A. Pebdani and S. Khodadoust, Design of an efficient uranyl ion optical sensor based on 1′-2,2′-(1,2-phenylene)bis(ethene-2,1-diyl)dinaphthalen-2-ol, *Mater. Sci. Eng. C*, 2012, **32**, 1888-1892.

57 M. Shamsipur, J. Tashkhourian and H. Sharghi, Development of a PVC-membrane ion-selective bulk optode, for UO_2^{2+} ion, based on tri-n-octylphosphine oxide and dibenzoylmethane, *Anal. Bioanal. Chem.*, 2005, **382**, 1159-1162.

58 Y. Kalyan, A. Pandey, G. Naidu and A. Reddy, Membrane optode for uranium (VI) ions preconcentration and quantification based on a synergistic combination of 4-(2-thiazolylazo)-resorcinol with 8-hydroxyquinaldine, *Spectrochim. Acta A*, 2009, **74**, 1235-1241.

59 J. Joshi, P. Pathak, A. Pandey and V. Manchanda, Optode for uranium (VI) determination in aqueous medium, *Talanta*, 2008, **76**, 60-65.

Figure legends

Fig.1 Structure of 5-(9-anthracenylmethyl)-5-aza-2,8-dithia[9],(2,9)-1,10-phenanthrolinophane (L).

Fig. 2 Excitation (Ex) and emission (Em) spectra of 5.00×10^{-5} M of **L** in acetonitrile solution in the presence of increasing concentration of uranyl ion: (1) 0.00, (2) 3.13×10^{-6} M, (3) 6.25×10^{-6} M, (4) 9.38×10^{-6} M, (5) 1.25×10^{-5} M, (6) 1.56×10^{-5} M (7), 1.88×10^{-5} M, (8) 2.19×10^{-5} M, (9) 2.50×10^{-5} M, (10) 2.81×10^{-5} M, (11) 3.13×10^{-5} M, (12) 3.75×10^{-5} M, (13) 4.38×10^{-5} M, (14) 5.00×10^{-5} M, (15) 7.50×10^{-5} M, (16) 1.00×10^{-4} M.

Fig. 3 Fluorescence intensity versus [metal]/[ligand] molar ratio plots in acetonitrile solution: (1) UO_2^{2+}, (2) Al^{3+}, (3) La^{3+}, (4) Ce^{3+} (5) Pr^{3+}, (6) Sm^{3+}, (7) Ag^{+}, (8) Cd^{2+}, (9) Hg^{2+}, (10) Pb2+.

Fig. 4 Optimized structures of free **L** (A) and its $[UO_2(\mathbf{L})_2]^{2+}$ complex (B).

Fig. 5 Excitation and emission spectra of the uranyl-selective optical sensor in the presence of increasing concentrations of uranyl ion: (1) buffer solution of pH 4.0, (2) 1.0×10^{-11} M, (3) 1.0×10^{-10} M, (4) 1.0×10^{-9} M, , (5) 1.0×10^{-8} M, (6) 1.0×10^{-7} M, (7) 1.0×10^{-6} M, (8) 1.0×10^{-5} M, (9) 1.0×10^{-4} M, (10) 1.0×10^{-3} M, (11) 1.0×10^{-2} M,

Fig. 6 Effect of pH on the response of membrane in the presence of 1.0×10^{-6} M uranyl ion.

Fig. 7 Relative fluorescence intensity (1-α) as a function of p-uranyl. The curves fitting the experimental data were calculated from Eq. (6). Data points experimentally obtained (blue dots), m:n = 1:1 (red line), m:n = 1:2 (blue line), m:n = 2:1 (purple line).

Fig.8 Interference of 1.0×10^{-4} M of different cations on the fluorescence determination of 1.0×10^{-6} M uranyl ion with the proposed membrane sensor.

Table 1 Formation constants of different 1:2 M^{n+}:**L** complexes in Acetonitrile solution

Metal ion	Log K_f
Uranyl	12.79±0.04
Al(III)	8.42±0.05
La(III)	6.27±0.05
Ce(III)	4.81±0.04
Pr(III)	4.63±0.03
Sm(III)	4.54±0.04
Ag(I)	3.96±0.04
Cd(II)	3.75±0.04
Hg(II)	3.29±0.05
Pb(II)	3.03±0.04

Table 2 Optimization of membrane ingredients

No.	PVC (mg)	Plasticizer (mg)	NaTPB (mg)	**L** (mg)	Dynamic range (M)
1	31	60 (NPOE)	2	7	1.0×10^{-10}-1.0×10^{-3}
2	31	60 (TEHP)	2	7	5.6×10^{-7}-8.3×10^{-5}
3	31	60 (DOS)	2	7	2.3×10^{-6}-2.4×10^{-4}
4	31	60 (DOP)	2	7	3.9×10^{-7}-3.5×10^{-4}
5	31	60 (DBP)	2	7	6.2×10^{-8}-7.2×10^{-5}
6	33	60 (NPOE)	2	5	1.3×10^{-9}-8.7×10^{-4}
7	29	60 (NPOE)	2	9	7.6×10^{-10}-2.9×10^{-5}
8	34	60 (NPOE)	1	5	9.2×10^{-9}-3.4×10^{-5}
9	32	60 (NPOE)	3	5	8.8×10^{-9}-2.7×10^{-5}
10	38	60 (NPOE)	2	0	7.5×10^{-6}-3.1×10^{-4}

Table 3 Determination of uranyl in water samples at the optimum conditions (n=5)

Sample	Added (M)	Found (M)	RSD (%)	Recovery (%)	t-test[a]
1	0	< DL	—	—	—
2	3.0×10^{-5}	$(2.93\pm0.10)\times10^{-5}$	3.41	97.67	1.56
3	6.0×10^{-7}	$(6.16\pm0.18)\times10^{-7}$	2.92	102.67	1.99
4	9.0×10^{-9}	$(8.75\pm0.27)\times10^{-9}$	3.09	97.22	2.07

[a] Tabulated t-value at P = 0.05 is 2.31.

Table 4 Determination of uranyl in uranium mines samples at the optimum conditions (n=3)

Sample	Added (ppm)	Found by ICP-AES (ppm)	Found by proposed sensor (ppm)	RSD (%)	Recovery (%)
1	0	62.4 ± 0.3	62.0 ± 0.6	0.97	99.36
2	30	93.7 ± 0.4	94.1 ± 0.9	0.96	100.43
3	60	121.5 ± 0.6	120.8 ± 1.1	0.91	99.42
4	90	152.2 ± 0.7	152.4 ± 1.5	0.98	100.13

Table 5 Analysis of uranyl in mixed cation solutions by proposed sensor (n=3)

Composition (%)	Uranyl added (%)	Uranyl found (%)	t-test[a]
(1) Hg^{2+}, 25 ; Ag^{+}, 25 ; Cd^{2+}, 25 ; Zn^{2+}, 24 ; UO_2^{2+}, 1	1.00	1.02 ± 0.03	1.15
(2) Al^{3+}, 20 ; La^{3+}, 20 ; Ce^{3+}, 20 ; Pr^{3+}, 20 ; Sm^{3+}, 19 ; UO_2^{2+}, 1	1.00	1.04 ± 0.04	1.73

[a] Tabulated t-value at P = 0.05 is 2.31.

Table 6 Comparison of the response characteristics of the proposed uranyl optode with the previously reported optical sensors

Ref.	Response time (min)	Dynamic range (M)	pH	Detection limit (M)
14	12	2.5×10^{-8}–4.3×10^{-6}	4.0	8.0×10^{-9}
53	6	1.7×10^{-5}–1.9×10^{-4}	4.5	5.0×10^{-6}
54	5	1.0×10^{-8}–1.0×10^{-6}	5.0	6.0×10^{-9}
55	8	1.0×10^{-6}–1.5×10^{-4}	5.5	8.2×10^{-7}
56	10	4.0×10^{-6}–8.1×10^{-8}	3.0	1.0×10^{-6}
57	8	4.1×10^{-6}–2.0×10^{-4}	4.0	2.5×10^{-6}
58	30	1.0×10^{-8}–1.1×10^{-7}	4.7	1.0×10^{-8}
59	30	1.5×10^{-6}–1.5×10^{-5}	7.0	1.1×10^{-6}
This work	3	1.0×10^{-10}–1.0×10^{-3}	4.0	2.7×10^{-11}

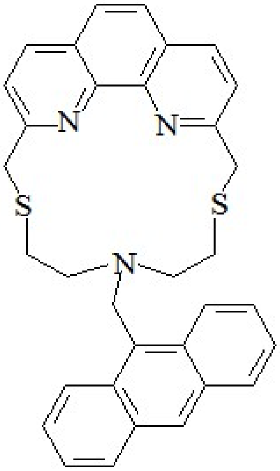

Fig.1

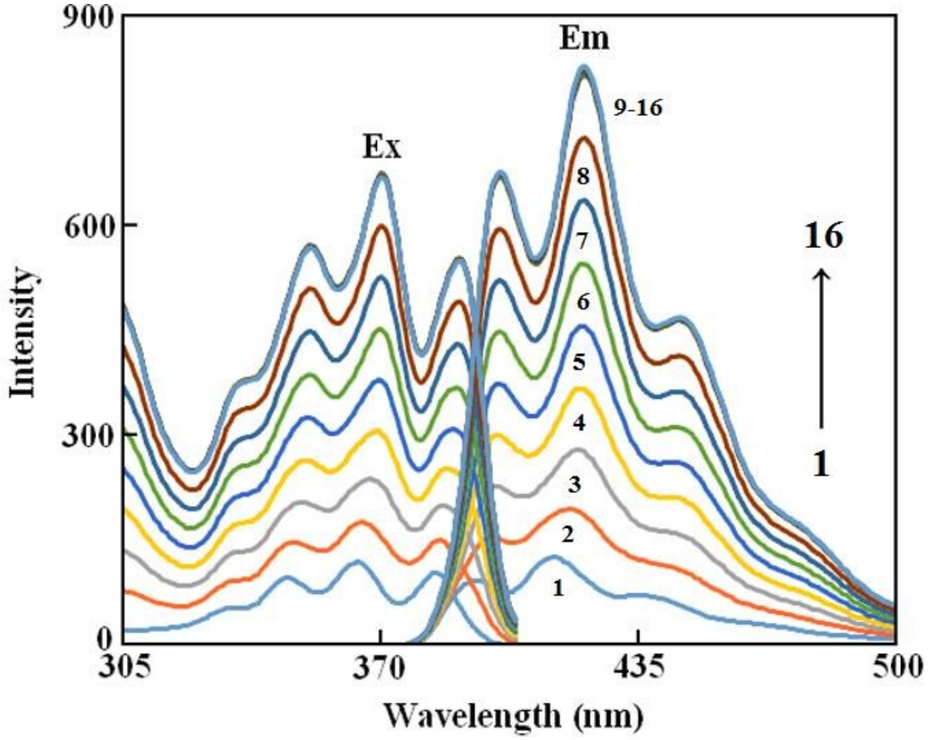
Em
9-16
Ex
8
7
6
5
4
3
2
1
16
1
Intensity
900
600
300
0
305
370
435
500
Wavelength (nm)

Fig. 2

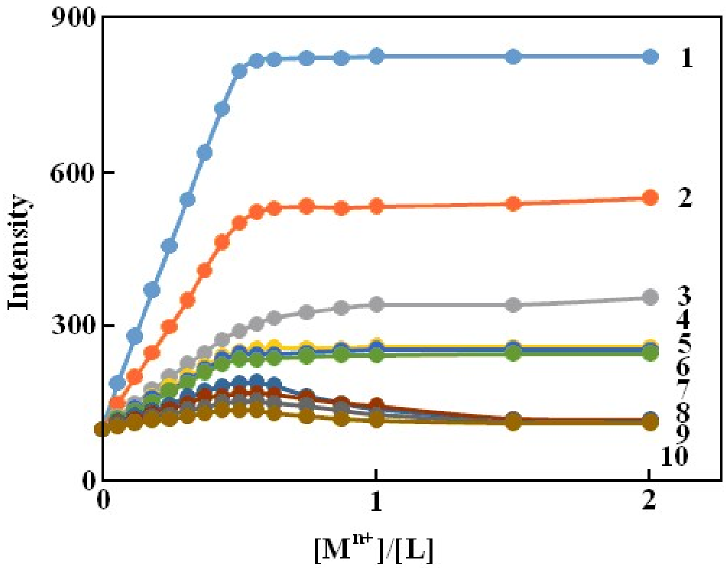

Fig. 3

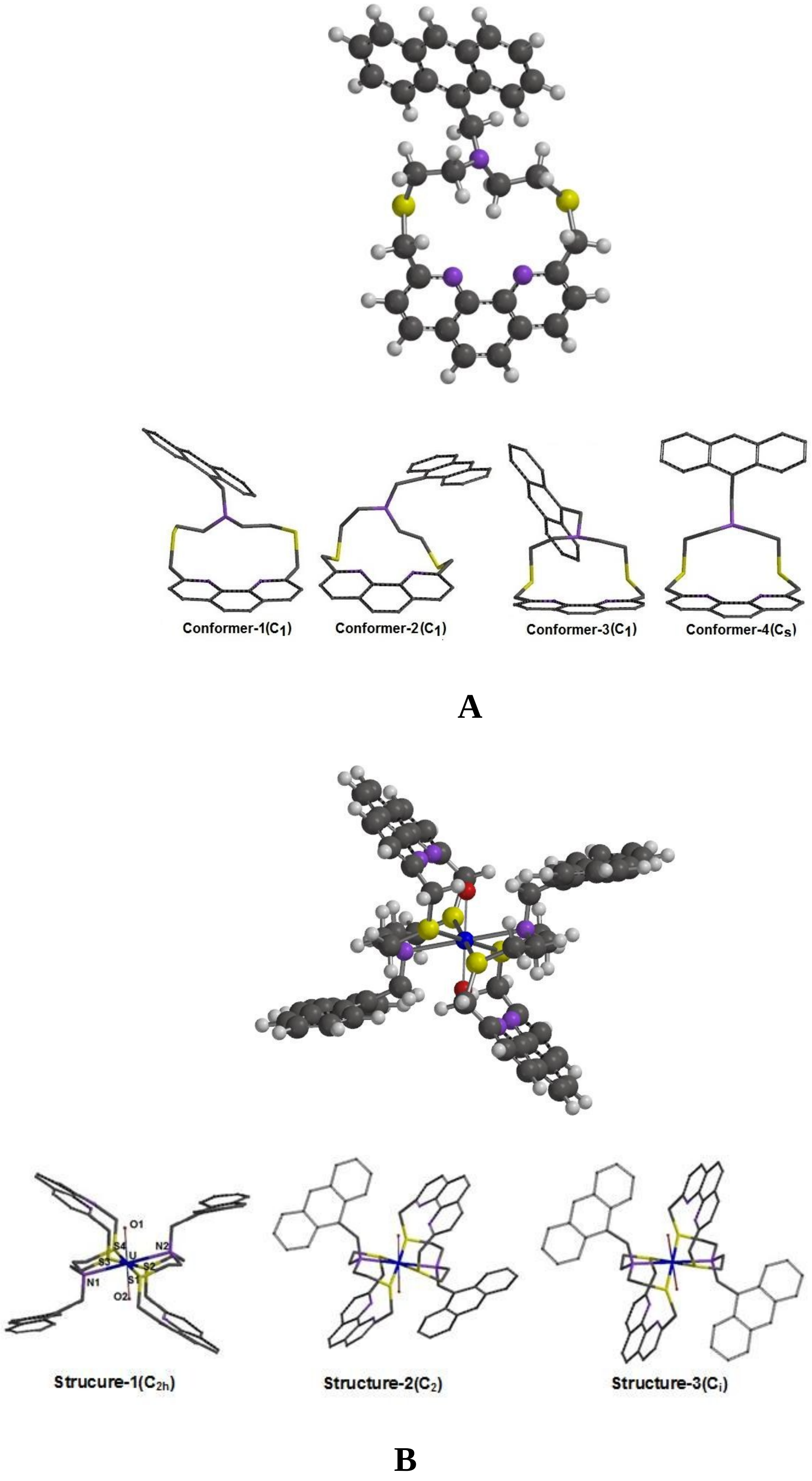
Conformer-1(C1)
Conformer-2(C1)
Conformer-3(C1)
Conformer-4(Cs)
A
O1
S4
S3
U
N2
N1
S1
S2
O2
Strucure-1(C2h)
Structure-2(C2)
Structure-3(Ci)
B

Fig. 4

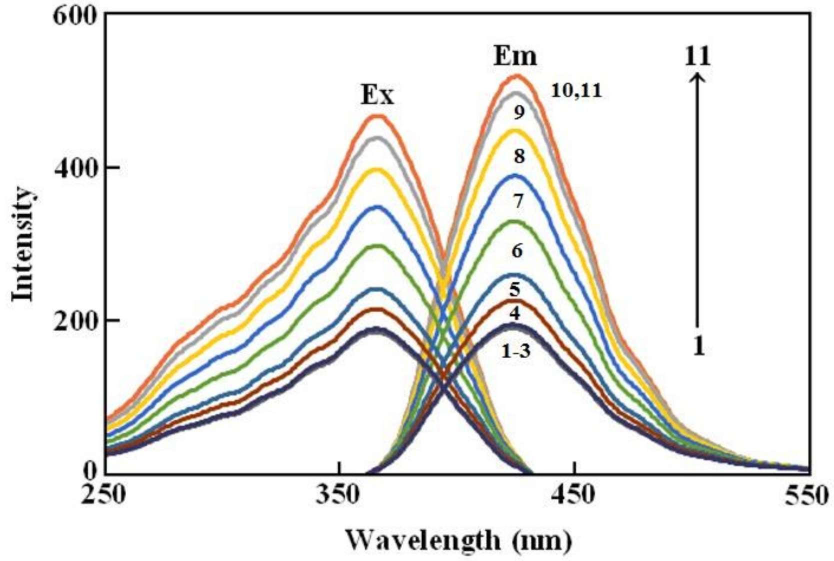
600
400
200
0
Intensity
250
350
450
550
Wavelength (nm)
Ex
Em
10,11
9
8
7
6
5
4
1-3
11
1

Fig. 5

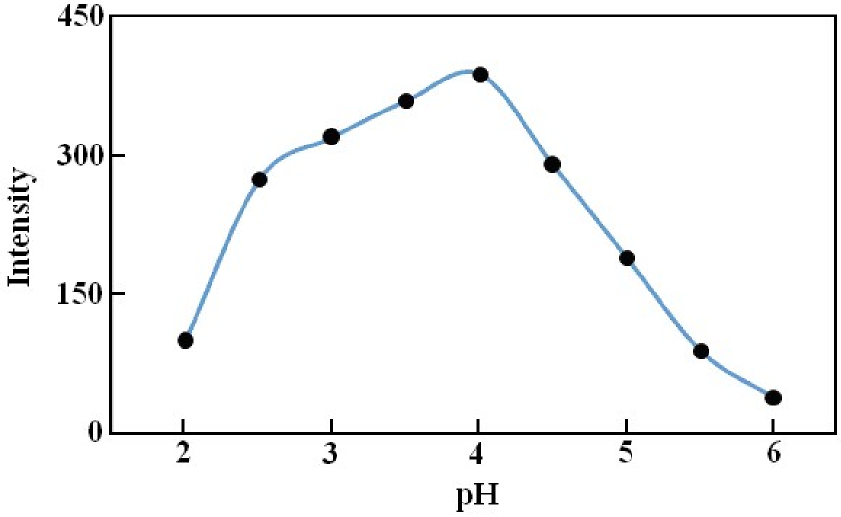

Fig. 6

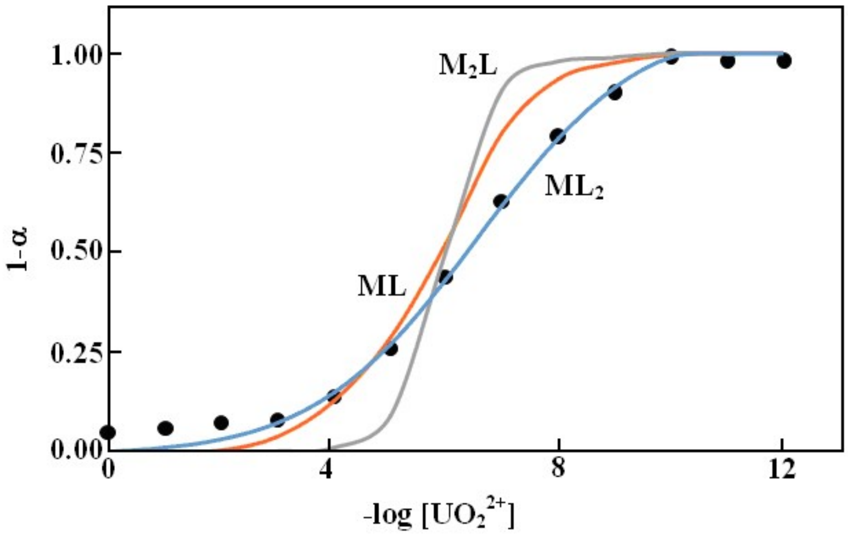

Fig. 7

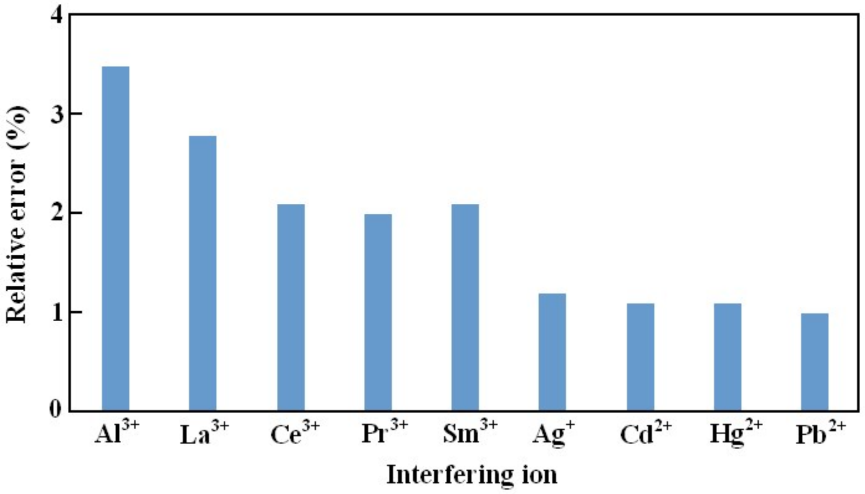
Relative error (%)
0
1
2
3
4
Al^{3+}
La^{3+}
Ce^{3+}
Pr^{3+}
Sm^{3+}
Ag^{+}
Cd^{2+}
Hg^{2+}
Pb^{2+}
Interfering ion

Fig. 8